Demonstration of Differential Post-Stenotic Myocardial Technetium-99m-Teboroxime Clearance Kinetics After Experimental Ischemia and Hyperemic Stress

Richard E. Stewart, Betty Heyl, Robert A. O'Rourke, Ralph Blumhardt, and D. Douglas Miller

Department of Medicine, Division of Cardiology, and Department of Radiology, Division of Nuclear Medicine, University of Texas Health Science Center, San Antonio, Texas

The clearance kinetics of the perfusion tracer ^{99m}Tc-teboroxime were evaluated in post-stenotic and normal myocardium using dynamic planar gamma camera imaging in pre-instrumented dogs in the control state (n = 9) and following total occlusion (2 min), pharmacologic stress with adenosine [80 and 160 μg/kg/min] or dipyridamole, and rapid atrial pacing (220/min). Technetium-99m-teboroxime clearance in normal myocardium was accelerated by adenosine and by dipyridamole compared to the control state (8.9 ± 1.1 and 9.3 ± 1.9 min versus 11.9 ± 1.8 min; $p < 0.05$). Post-stenotic ^{99m}Tc-teboroxime clearance half-time was most significantly prolonged compared to nonoccluded contralateral perfusion zones by 160 μg/kg/min adenosine stress (11.2 ± 3.7 versus 6.3 ± 1.5 min) and by complete coronary occlusion (12.1 ± 3.3 versus 6.6 ± 1.2 min; both $p < 0.05$). Differential tracer clearance from post-stenotic versus nonoccluded zones produced quantitative evidence of relative defect "redistribution" in 71% of maximal stress studies at a mean of 8.8 ± 2.5 min postinjection. Sensitivity, specificity, and diagnostic accuracy of prolonged regional ^{99m}Tc-teboroxime clearance rates for post-stenotic perfusion abnormalities were 62%, 100% and 81% in maximal stress studies. Future clinical trials of exercise and nonexercise stress ^{99m}Tc-teboroxime imaging should consider these kinetic characteristics and examine the correlates of perfusion defect "redistribution."

J Nucl Med 1991; 32:2000–2008

Technetium-99m-teboroxime (methyl-boron [1-]-tris [1,2-cyclohexane dione dioxime (1-)]-N′,N″,N‴, N⁗,N⁗′) chlorotechnetium is a rapidly cleared myocardial perfusion agent currently being evaluated in exercise-rest protocols in patients with suspected ischemic heart disease (*1–3*). These early clinical trials of exercise ^{99m}Tc-teboroxime imaging have shown comparable diagnostic accuracy to ^{201}Tl SPECT for detection of significant coronary artery disease (*4*). Serial ^{99m}Tc-teboroxime imaging after pharmacologic or atrial pacing stress would extend the clinical diagnostic utility of this new imaging agent to include patients unable to exercise. Post-reperfusion ^{99m}Tc-teboroxime imaging during interventional procedures would theoretically permit the earlier detection of ischemic myocardium in an acute care setting.

Myocardial uptake of ^{99m}Tc-teboroxime is rapid, with high extraction fraction over a wide range of flows (*5*) and diagnostic quality cardiac visualization within 2 min of injection (*5,6*). In animal studies, tracer clearance is closely related to myocardial blood flow (*5*). Preliminary clinical studies (*2*) indicate that serial dynamic myocardial perfusion imaging may be achievable with this agent.

The goal of the present study was to compare the kinetic behavior of ^{99m}Tc-teboroxime in normal and post-stenotic myocardium in response to occlusive ("supply"), rapid pacing ("demand"), and pharmacologic ("hyperemic") stress in the intact pre-instrumented canine model. This animal model simulates relevant clinical situations and permits the serial acquisition of detailed hemodynamic data to correlate with the in vivo myocardial kinetics of this new perfusion agent.

The hypothesis that post-stenotic ^{99m}Tc-teboroxime myocardial clearance varies with different types of ischemic cardiac stress was tested. In addition, the corollary of whether rapid differential myocardial clearance of ^{99m}Tc-teboroxime predisposes early tracer "redistribution" in post-stenotic myocardium was also examined.

METHODS

Technetium-99m-Teboroxime Radiopharmaceutical Preparation

Kits containing vials of lyophilized ^{99m}Tc-teboroxime were supplied by Squibb Diagnostic Division, Princeton, NJ. Technetium-99m-sodium pertechnetate was obtained from ^{99}Mo/^{99m}Tc generators that were eluted within 24 hr of radiopharmaceutical preparation. Radionuclide purity, aluminum ion content, and pH were determined prior to use.

Received Oct. 26, 1990; revision accepted Jan. 29, 1991.

For reprints contact: D. Douglas Miller, MD, Department of Medicine, Division of Cardiology, St. Louis University Medical Center, 3635 Vista Ave., St. Louis, MO 63110-0250

Each vial was reconstituted with 1 ml of [^{99m}Tc]sodium pertechnetate, containing approximately 2–4 mCi of radioactivity. The radiochemical purity was determined utilizing 1.3 × 11 cm Whatman 31 ET chromatography strips and two individual mobile face solvent systems. Chromatographic results indicated that the sum of the free ^{99m}Tc and reduced/hydrolyzed ^{99m}Tc-teboroxime was routinely less than 10%, while the mean radiochemical purity averaged greater than 95%.

Hemodynamic Data Acquisition and Analysis

Healthy mongrel dogs (15–20 kg) were surgically pre-instrumented for chronic physiologic monitoring using a previously reported method (*7*). High fidelity left ventricular (LV) pressure (LV end-diastolic pressure), the first derivative of LV pressure [dP/dt], aortic pressure, the minor axis LV dimension, apical and basal regional segment lengths and a surface ECG were recorded on internally grounded an eight channel forced ink pen oscillograph [Beckman Instruments, Inc., Fullerton, CA] at a paper speed of 25 mm/sec. An average of 15 to 20 consecutive cardiac cycles were recorded for on- or offline analysis using software developed in our laboratory. Percent regional LV systolic shortening [%SS] was calculated according to a previous published method (*7,8*). These parameters were used to establish the presence and define the time of peak LV hemodynamic stress.

Experimental Protocol

All animals were anesthetized with intravenous pentobarbital [30 mg/kg] in the right lateral decubitus position for the duration of the studies. All nine dogs (five pre-instrumented with coronary artery occluders and four pre-instrumented without occluders) underwent imaging with 10 ± 1 mCi of ^{99m}Tc-teboroxime under baseline conditions (without occluders inflated). Experimental stress runs were carried out in random order in each of the five occluded dogs after either 5 min of partial [≥90%] single-vessel coronary artery occlusion or 2 min of complete [100%] occlusion. A minimum interval of 48 hr was allowed between serial studies to permit full hemodynamic recovery. Following partial (≥90%) coronary occlusion, the dogs underwent the following pharmacologic stress: 80 μg/kg/min or 160 μg/kg/min adenosine (Sigma, Inc., St. Louis, MO) intravenously for 3 min, or dipyridamole (Boehringer Ingelheim, Ridgefield, CT) 0.14 mg/kg/min intravenously over 4 min (total dose = 0.56 mg/kg).

"Demand" ischemia was achieved with partial occlusion and atrial pacing at 220 bpm. Technetium-99m-teboroxime was administered as an intravenous bolus (flushed with 10 ml of normal saline) at the point of peak stress as defined by online LV hemodynamics. This occurred at 2 ± 1 min following the onset of adenosine infusion and at 7 ± 1 min following initiation of dipyridamole infusion. Experimental runs were also performed as described above without coronary artery occlusion.

Image Acquisition and Analysis

Image acquisition was performed using a Searle MEDX-37 gamma camera fitted with a low-energy all-purpose collimator and interfaced with a Medisys A^2 computer (matrix = 64 × 64 byte; zoom = 1.69). A 20% automatic photopeak window was set around 140 keV. All images were acquired in the 50° left anterior oblique camera position. Image acquisition was started at the time of injection and consisted of 40 frames (30 sec per frame) followed by 2 frames of 5 min per frame. Total imaging time per study was 30 min. Animals were repositioned for serial imaging studies by placing the thoracotomy incision scar at the level of the midpoint of the camera-collimator surface (determined by cross-hatched markings).

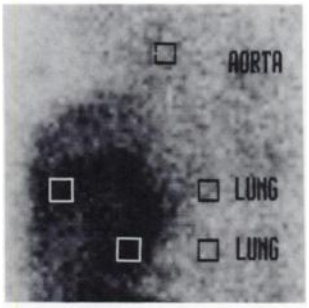

FIGURE 1. ROIs for analysis of myocardial, blood-pool and lung activity are demonstrated at 1.5 min postinjection. Myocardial ROIs were set in the anteroseptal and posterolateral regions (white boxes), distant from the apical instrumentation "dimple." Two lung ROIs were placed at the same level as the myocardial ROIs, well above the splanchnic activity. Blood-pool ROIs were placed in the central ventricular cavity (LV) and in the ascending aorta (Aorta).

Twenty-five pixel regions of interests (ROI) were drawn by two independent observers in the post-stenotic and nonoccluded (normal) myocardium corresponding to the anteroseptal and posterior myocardial walls (Fig. 1). Background ROIs were placed over two lung regions at the level of the LV chamber, and the LV cavity and ventricular outflow tract. All regions were fixed for the duration of studies, but could be adjusted for animal motion. Care was taken to minimize the contribution of hepatobilary activity to the inferoposterior wall using adjustments in camera position guided by an activity source before ^{99m}Tc-teboroxime injection. Systematic prospective evaluation of the contribution of all four background ROIs to myocardial activity was performed in representative control and stress studies. An average of the LV outflow tract and one lung region produced optimum correction for both early (0–2 min) blood-pool and later (2–11 min) lung background activity adjacent to the myocardial ROIs. Data from each individual image frame were decay-corrected and background-subtracted using a method similar to those previously reported for analysis of dynamic myocardial radioisotope clearance with serial planar imaging (*9,10*).

Technetium-99m time-activity curves were initially expressed as raw mean counts/pixel/30-sec frame and fitted to the biexponential equation: $Y = ae^{-\lambda 1 t1} + be^{-\lambda 2 t2}$ (see reference *31*). Tracer clearance half-times [$t_{½}$ in minutes] were derived by linear regression of the natural logarithmic transformation of the decay corrected and background subtracted ^{99m}Tc raw myocardial time-activity curves acquired during the first 11 min of each study, according to the standard equation: $t_{½} = \ln 2/\lambda_1$ (*4,5*).

Relative "redistribution," the apparent normalization of ^{99m}Tc-teboroxime activity in post-stenotic myocardial defects, was assessed qualitatively and quantitatively. Serial planar images (30-sec studies × 20 min) were visually scored by two observers blinded to both the study and experimental protocol for qualitative reduction of defect size (i.e., "redistribution") (*11*). Quantitative "redistribution" ("R") was prospectively defined as the point at which the log transformed 1–11-min time-activity curves [post-stenotic zone (curve A–C) versus normal zone (curve B–D)] reached ≤40% of their initial (time = 1 min) count density difference (Fig. 2) (*12*):

$$"R"_{(1-11)} = \frac{(C - D)_{11}}{(A - B)_1} \leq 0.40$$

where "R" = quantitative "redistribution", A = ln post-stenotic myocardial counts (time 1 min), B = ln normal zone counts

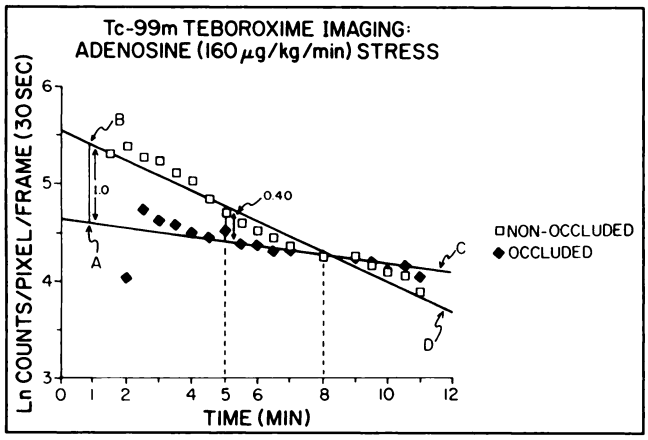

FIGURE 2. Log transformed myocardial clearance data from a study of severe partial coronary stenosis during adenosine [160 μg/kg/min] stress. The approach of the normal zone (curve B–D) and post-stenotic zone (curve A–C) clearance curves at point C–D to within 40% of their initial 1-min difference at point A–B occurs at 5 min (6 min postinjection). These curves intersect at 8 min postinjection. Quantitative relative "redistribution" was accompanied by qualitative partial "fill-in" of the anteroseptal perfusion defect. The myocardial clearance half-time in the non-occluded zone was 4.9 min as compared to 10.5 min in the post-stenotic zone.

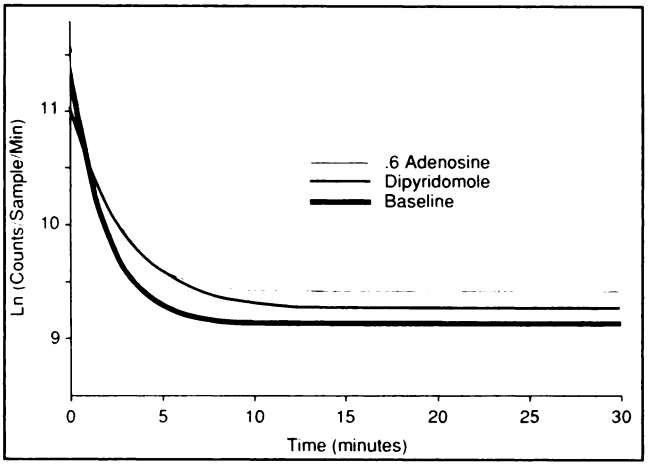

FIGURE 3. Systemic arterial blood clearance of ^{99m}Tc-teboroxime was evaluated in the subset of 3 dogs instrumented for Doppler coronary artery blood flow determination. Tracer clearance was biexponential under baseline conditions (k_1 = 1.29 ± .05, k_2 = 0.025 ± .004) and following pharmacologic stress with high-dose adenosine (k_1 = 1.68 ± .07, k_2 = 0.031 ± .003 and dipyridamole (k_1 = 1.82 ± .09, k_2 = 0.043 ± .004). Early blood ^{99m}Tc-teboroxime clearance kinetics were comparable and significantly different from control following dipyridamole and adenosine stresses.

(time 1 min), C = ln post-stenotic myocardial counts (time 11 min), and D = ln normal zone counts (time 11 min).

The choice of 11 min (10 min following the 0–1 min clearance of blood pool) was based on careful analysis of the raw data which routinely demonstrated a "breakpoint" between early and late washout at <11–12 min postinjection (see Fig. 4). Myocardial activity beyond 11 min postinjection was too low (27%–34% of 1 min postinjection), and clearance too statistically variable (late $t_{1/2}$ = 20 ± 2–33 ± 4 min) to permit further assessment of ^{99m}Tc-teboroxime clearance.

Statistical Analysis

Data are expressed as mean ± 1 s.d. Paired samples were compared using the Students t-test. A probability value of <0.05 was considered significant. Linear regression was calculated by the least squares method. Blood clearance data (Fig. 3) were fit to a biexponential function using the RS/1 software package "fit function" (Bolt, Baranek and Newman, Cambridge, MA).

RESULTS

Hemodynamic Response

Table 1 lists the hemodynamic responses at baseline and after peak pharmacologic and pacing stress. The peak stress triple product (heart rate × LV systolic pressure × $+dP/dt_{max}$) did not increase significantly after adenosine and dipyridamole infusion, consistent with previous studies of these pharmacologic stress agents on canine LV performance (*13*). There was a significant increase in cardiac index (7.1 ± 1.0 to 13.9 ± 4.6 l/min/m^2; $p < 0.05$) and triple product (43,578 ± 14,460 to 84,979 ± 35,431 units; $p < 0.05$) during pacing stress. The left ventricular end-diastolic pressure (LVEDP) increased only during complete occlusion (7 ± 4 to 21 ± 13 mmHg; $p < 0.05$).

Regional Contractile Function

The LV percent systolic shortening (%SS), an index of regional contractile function (*13*), is given in Table 2 for the post-stenotic and nonoccluded vascular beds. Total coronary occlusion, and partial occlusion with high-dose adenosine (160 μg/kg/min), dipyridamole or rapid atrial pacing transiently decreased post-stenotic LV contractile performance (all $p < 0.05$), which returned to normal at 10 min post-stress. Low-dose adenosine (80 μg/kg/min) plus stenosis did not depress post-stenotic LV contractile function.

Coronary blood flow was not directly measured in the presence of flow limiting stenoses. However, previously reported data from our laboratory (*19*) demonstrate a significant reduction in radiolabeled microsphere regional myocardial blood flows with severe (≥90%) partial stenosis alone (1.4–0.9 ml/min/g), partial stenosis and rapid atrial pacing (0.6 ml/min/g), and complete occlusion (0.2 ml/min/g; all $p < 0.05$).

Technetium-99m-Teboroxime Myocardial Clearance Kinetics

Table 3A summarizes the early (1–11 min) clearance half-times of ^{99m}Tc-teboroxime at control and under the varied stress conditions. Mean early ^{99m}Tc-teboroxime clearance was delayed in ischemic post-stenotic zones compared to contralateral normal myocardial zones under all conditions of pharmacologic and pacing stress ($p < 0.05$), but was most prolonged after the infusion of 160 μg/kg/min (11.2 ± 3.7 versus 6.3 ± 1.5 min; $p < 0.05$) (Fig. 4). There was also a significant difference in post-stenotic

TABLE 1
Hemodynamic Data

	I. Pharmacologic Stress (n = 5)					
	0.3 Adenosine		0.6 Adenosine		Dipyridamole	
	Baseline	Peak stress	Baseline	Peak stress	Baseline	Peak stress
HR	125 ± 26	157 ± 24	136 ± 43	172 ± 28	146 ± 24	174 ± 18
LVP systolic	123 ± 14	122 ± 12	138 ± 20	140 ± 12	126 ± 18	134 ± 22
LVEDP	5.6 ± 3.2	8.4 ± 7.4	7.0 ± 4.4	6.8 ± 9.5	5.8 ± 3.3	4.4 ± 12.8
$+dP/dt_{max}$	3,177 ± 1,077	3,475 ± 1,232	3,614 ± 954	4,443 ± 973	3,540 ± 965	4,706 ± 1,137
Triple product	53,373 ± 37,126	68,788 ± 35,760	75,290 ± 44,046	110,125 ± 39,000	83,558 ± 40,841	115,983 ± 47,174
Cardiac index	7.5 ± 1.0	8.9 ± 1.3	7.8 ± 1.8	9.8 ± 2.1	7.9 ± 1.6	12.0 ± 4.6

	II. Pacing Stress (n = 5)	
	Baseline	Peak stress
HR	106 ± 20	209 ± 9*
LVP systolic	120 ± 16	119 ± 21
LVEDP	6.8 ± 3.3	24 ± 7.0
$+dP/dt_{max}$	3370 ± 748	3327 ± 971
Triple product	43,580 ± 14,468	84,978 ± 35,432*
Cardiac index	7.1 ± 1.0	13.9 ± 4.6*

	III. Total Occlusion (n = 6)	
	Baseline	Peak stress
HR	124 ± 19	164 ± 20
LVP systolic	124 ± 11	108 ± 17
LVEDP	9.6 ± 3.3	21.2 ± 13.2*
$+dP/dt_{max}$	3,108 ± 327	2,389 ± 759
Triple product	47,866 ± 8,208	38,031 ± 16,094
Cardiac index	7.6 ± 1.8	6.6 ± 2.0

* $p < 0.05$ versus baseline.

LVP = LVP pressure (mmHg), LVEDP = LV end-diastolic pressure (mmHg), $+dP/dt_{max}$ = first derivative of LVP (mmHg/sec), and cardiac index = $l/min/m^2$.

clearance half-time between pacing stress (7.3 ± 1.2 min) and complete occlusion (12.1 ± 3.3 min; $p < 0.05$). Technetium-99m-teboroxime clearance in nonoccluded zones differed significantly from the control value (11.9 ± 1.8 min, $p < 0.05$) under all cardiac stress conditions.

Quantitative post-stenotic counts ratio analysis confirmed optimal defect visualization at 5 min postinjection (Table 3B). Lung:heart ^{99m}Tc-teboroxime activity ratios 5 min postinjection did not differ under varied experimental stress conditions.

TABLE 2
Percent Systolic Shortening Data

	Post-Stenotic bed			Nonoccluded bed		
Experimental conditions	Baseline	Peak	10 min postinjection	Baseline	Peak	10 min postinjection
No occlusion						
Control (n = 9)	13.3% ± 3.9%	—	—	13.0% ± 3.4%	—	—
0.6 Adenosine (n = 4)	12.7% ± 5.2%	12.4% ± 6.0%	12.3% ± 2.9	10.0% ± 4.2%	10.2% ± 4.0%	10.5% ± 1.8%
Dipyridamole (n = 4)	11.0% ± 5.9%	11.5% ± 6.5%	9.7% ± 4.9%	16.2% ± 1.9%	20.8% ± 7.8%	13.8% ± 4.3%
Total occlusion (n = 6)	15.5% ± 4.3%	10.4 ± 3.9%*	14.2% ± 3.4%	—	—	—
Partial occlusion (n = 5)						
+ Adenosine (0.3)	10.4% ± 4.8%	8.0% ± 3.7%	12.2% ± 4.6%	11.6% ± 4.1%	11.6% ± 4.2%	10.6% ± 3.5%
+ Adenosine (0.6)	11.2% ± 4.7%	7.6% ± 3.2%*	13.1% ± 5.9%	10.6% ± 4.1%	11.9% ± 5.0%	10.0% ± 3.9%
+ Dipyridamole	12.2% ± 3.6%	8.6% ± 4.8%*	11.5% ± 5.8%	15.4% ± 4.0%	19.1% ± 7.6%	15.0% ± 4.0%
+ Pacing (220/min)	12.3% ± 5.7%	8.1% ± 4.7%*	13.0% ± 3.5%	12.8% ± 2.7%	13.9% ± 5.5%	13.9% ± 4.7%

* $p < 0.05$ vs. baseline and 10′ post-values.

TABLE 3A
Technetium-99m-Teboroxime Imaging Data in Response to Pharmacologic and Ischemic Stress

	n	Myocardial clearance half-time (min)	
Control	9‡	11.9 ± 1.8	
No occlusion			
Adenosine (0.6)	5	8.9 ± 1.1	
Dipyridamole	5	9.3 ± 1.9	
Partial occlusion			
		Post-Stenotic zone	Normal zone
Adenosine (0.3)	5	10.6 ± 2.5*	7.0 ± 1.9†
Adenosine (0.6)	5	11.2 ± 3.7*	6.3 ± 1.5†
Dipyridamole	5	8.6 ± 2.1*	5.8 ± 1.4†
Pacing	5	7.3 ± 1.2*	5.6 ± 1.1†
Complete occlusion			
	6§	12.1 ± 3.3*	6.6 ± 1.2†

* $p < 0.05$ between post-stenotic and normal zone half-time.
† $p < 0.05$ vs. control half-time.
‡ Five pre-instrumented and four uninstrumented control dogs.
§ Six experimental runs in five dogs.

TABLE 3B
Technetium-99m-Teboroxime Imaging Data in Response to Pharmacologic and Ischemic Stress

	n	Myocardial Post-stenotic:normal zone counts ratio	
		5 min	10 min
Control	9†	0.87 ± 0.08	0.89 ± 0.11
No occlusion			
Adenosine (0.6)	5	0.87 ± 0.10	0.89 ± 0.10
Dipyridamole	5	0.89 ± 0.09	0.89 ± 0.10
Partial occlusion			
Adenosine (0.3)	5	0.70 ± 0.13	0.73 ± 0.18
Adenosine (0.6)	5	0.65 ± 0.12*	0.71 ± 0.17
Dipyridamole	5	0.73 ± 0.16*	0.74 ± 0.07
Pacing	5	0.70 ± 0.17	0.73 ± 0.22
Complete occlusion			
	6‡	0.82 ± 0.09	0.91 ± 23

* $p < 0.05$ vs. corresponding "no occlusion" counts ratio.
† Five pre-instrumented and four uninstrumented control dogs.
‡ Six experimental runs in five dogs.

Qualitative Versus Quantitative Analysis of ^{99m}Tc-Teboroxime Myocardial Redistribution

Two independent observers qualitatively graded myocardial visualization as good to excellent in 28 of 35 (80%) of all studies, and defect visualization as present in 22/26 (85%) of stress studies (Fig. 5). Figure 6 is an example of a post-stenotic myocardial perfusion defect with qualitative relative "redistribution" of ^{99m}Tc-teboroxime activity. The corresponding clearance curves are shown in Figure 2, with the curves reaching ≤40% of their original log transformed count density difference within 10 min of injection. Using this quantitative definition, relative "redistribution" was present in 71% of maximal stress studies [15/21]: 60% after pacing stress, 60% after pharmacologic stress with adenosine 160 μg/kg/min, 80% after dipyridamole stress and 83% after complete occlusion (n = 5/6 studies), and in 17/26 (65%) of all studies. Concordance between "redistribution" scoring by quantitative curve analysis and blinded expert qualitative scoring was 60%.

Diagnostic Accuracy for Detection of Abnormal ^{99m}Tc-Teboroxime Clearance

If normal ^{99m}Tc-teboroxime clearance is defined as <2 s.d. above the nonoccluded group mean, then the sensitivity of regional tracer clearance half-time determinations for detecting post-stenotic perfusion abnormalities in low- and high-dose adenosine, dipyridamole, pacing, stress, and total occlusion studies was 25%, 60%, 60%, 60%, and 66%, respectively. Overall sensitivity was 54% (14/26) including low-dose adenosine studies and 62% (13/21) excluding these sub-maximal adenosine studies. Six additional studies demonstrated visual evidence of relative "redistribution" but did not have regional clearance half-time values exceeding 2 s.d. above the mean. When combined with quantitative clearance data, qualitative scoring improved sensitivity to 60%, 80%, 100%, 60% and 66% in the above study groups; and 73% overall.

None of the 26 nonoccluded zones demonstrated half-time clearance rates exceeding 2 s.d. above the mean, producing no false-positives and a specificity of 100% using this criteria. The diagnostic accuracy was 77% for all types of stress in 52 segments and 81% in maximal stress studies analyzed for the presence of abnormal ^{99m}Tc-teboroxime clearance.

DISCUSSION

The current study utilized widely available dynamic planar gamma camera imaging in a validated pre-instrumented chronic dog model of severe coronary stenosis, with pacing and varied hyperemic stresses. The following observations were made:

1. Technetium-99m-teboroxime clearance is significantly delayed in ischemic myocardium distal to severe (≥90%) stenoses following rapid atrial pacing, adenosine and dipyridamole stresses as compared to the contralateral nonoccluded zone.
2. Increased cardiac work (i.e., triple product), high-dose adenosine (160 μg/kg/min) and dipyridamole infusion accelerate ^{99m}Tc-teboroxime clearance from nonoccluded zones compared to control data from the same perfusion beds.
3. High-dose adenosine stress and complete (100%) occlusion with reperfusion caused the greatest prolongation of teboroxime clearance compared to nonoccluded zones.
4. Differential post-stenotic versus nonoccluded zone

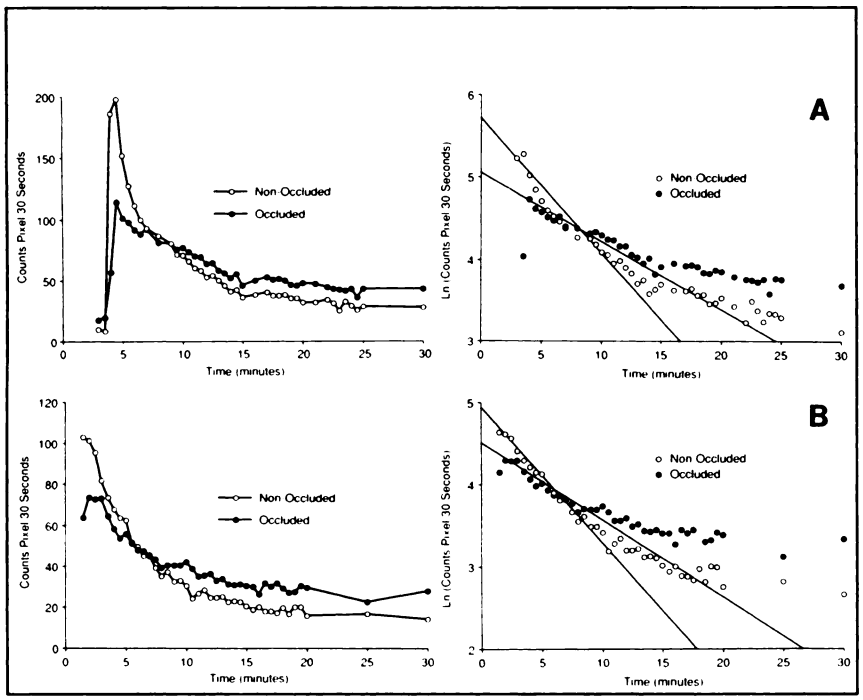

FIGURE 4. (A) Typical myocardial clearance kinetic data (0–30 min) following ^{99m}Tc-teboroxime injection (10 mCi i.v.) during high-dose adenosine stress. The post-stenotic zone (closed circles) and contralateral nonoccluded zone (open circles) data are derived from fixed ROIs in the anteroseptal and posterolateral myocardium. The raw kinetic data [upper left] and log transformed data [upper right] with corresponding regression curves are shown (r = 0.9). In this study, the early clearance half-time in the nonoccluded zone was 5 min as compared to 11 min in the post-stenotic ("occluded") perfusion bed. (B) Representative myocardial clearance kinetic data (0–30 min) following injection of ^{99m}Tc-teboroxime (10 mCi i.v.) in fixed myocardial ROIs in the occluded anteroseptal (closed circles) and nonoccluded posterolateral (open circles) perfusion beds following total (100%) occlusion of the left anterior descending coronary artery. The raw clearance data [lower left] and log transformed data [lower right] are displayed, with regression of the log transformed data (r = 0.9). The post-stenotic clearance half-time was delayed versus nonoccluded perfusion zones (11.5 vs 6.0 min).

^{99m}Tc-teboroxime myocardial clearance results in quantitative "redistribution" of activity into post-stenotic myocardium in 60%–83% (71% ± 12%) of studies at an average of 8.8 ± 2.5 min following injection, with qualitative evidence of defect "redistribution" in 60% of these studies.

5. Sensitivity, specificity, and diagnostic accuracy of tracer half-time clearance data for detecting post-stenotic perfusion abnormalities were 62%, 100% and 81% after maximal stress. These data acquired in a close-chested animal model may be extrapolated, with caution, to the clinical use of ^{99m}Tc-teboroxime myocardial perfusion imaging.

Myocardial Imaging Considerations

Myocardial Tracer Uptake. The peak myocardial uptake of intravenously injected ^{99m}Tc-teboroxime is 2.3% ± 0.8% of the injected dose (*1*), and is theoretically related to coronary blood flow (relative to cardiac output) and extraction fraction. In perfused hearts, myocardial extraction of this agent consistently exceeds that of either ^{201}Tl or ^{99m}Tc-sestamibi (mean E max = 0.76 ± .09 versus 0.62 ± 0.09 versus 0.30 ± .10; $p < 0.01$) (*20*). The myocardial extraction (E max = 0.72 ± 0.09) remains constant over a wide range of flows (*5,20*). Coronary blood flow was not directly measured during the stress-occlusion imaging studies, although Doppler flow probe studies in a subgroup of animals confirmed significant coronary hyperemia comparable to previous studies (*14–18*) in response to high dose adenosine (coronary flow reserve = 2.0) and dipyridamole (coronary flow reserve = 2.6) infusion. The ratio of increased coronary blood flow to cardiac output (1.6–4.4) favored myocardial tracer uptake during pharmacologic coronary vasodilation. Differences in the regional uptake of ^{99m}Tc-teboroxime following these varied stresses should therefore have been primarily dependent upon changes in regional myocardial blood flow.

Myocardial Clearance Kinetics. Canine studies have demonstrated differential washout rates of ^{99m}Tc-teboroxime during baseline conditions and coronary hyperemia within 4 min of injection using a modified SPECT camera system (*5*). This differential clearance effect is observed in both early ($t_{½}$ = 2.3 ± 0.6 versus 1.5 ± 0.6 min) and late ($t_{½}$ = 20 ± 9 versus 34 ± 9 min) phases of ^{99m}Tc-teboroxime washout. In a study utilizing serial planar imaging (*4*), postexercise ^{99m}Tc-teboroxime washout in both normal and CAD patients was faster than that occurring at rest. In CAD patients, late phase washout half-time following rest injection equalled 50 ± 17 min versus 31 ± 10 min in normal subjects ($p < 0.01$). Thus, the myocardial clearance of ^{99m}Tc-teboroxime occurs at different rates during coronary hyperemia and varied levels of cardiac work and may be delayed under conditions of chronic myocardial ischemia.

We made no attempt to perform compartmental analysis on these dynamic 30-sec images that do not possess the temporal resolution of our serial blood sampling data. Cardiac Na(Tl) probe studies of myocardial clearance of this agent following intracoronary injection demonstrate a biexponential washout pattern with a 2-min fast compo-

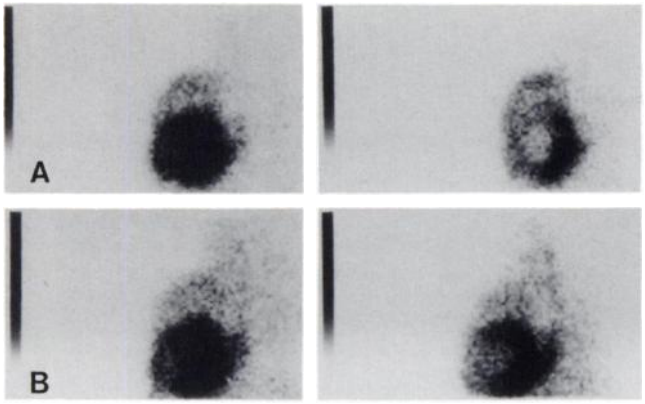

FIGURE 5. (A) Paired images following injection of ^{99m}Tc-teboroxime (10 mCi i.v.) during dipyridamole stress without stenosis [upper left], and dipyridamole stress with partial LAD occlusion [upper right]. The dipyridamole baseline study demonstrates excellent cardiac visualization with some residual blood-pool activity (1 min postinjection) and a small defect at the apical site of instrumentation. The stress image illustrates a myocardial perfusion defect in the anteroseptal wall. (B) A paired image set following injection of ^{99m}Tc-teboroxime (10 mCi i.v.) in the control state [lower left] without stress or coronary stenosis, and during pacing stress with partial LAD stenosis [lower right]. Myocardial visualization is excellent, with a small apical defect due to instrumentation in the "baseline" study. Pacing stress plus partial stenosis produced a transient anteroseptal wall motion abnormality in the LAD territory.

nent and a variable (20–78 min) slow component (*1,5*). Preliminary kinetic studies using high temporal resolution probe analysis of regional myocardial ^{99m}Tc-teboroxime activity in a canine occlusion model have confirmed bioexponential tracer clearance and differential washout in normal versus ischemic tissues (*31*). Low counts and statistical "noise" of the late (>11 min) counts made any determination of a late compartment size impossible. The reduction from 1-min postinjection peak average counts at 15–20 min following injection was 70% ± 30% (residual mean activity = 30% ± 3%). This deterioration of count rates was visually confirmed on inspection of these images.

Image-derived myocardial activity clearance after intravenous injection is monoexponential during control conditions and following dipyridamole stress (mean $t_{1/2}$ = 21 ± 4 versus 12 ± 4 min) (*5*). Differences in clearance kinetics following intracoronary and intravenous injection are due in part to tracer recirculation and continued reuptake postinjection following intravenous dosing.

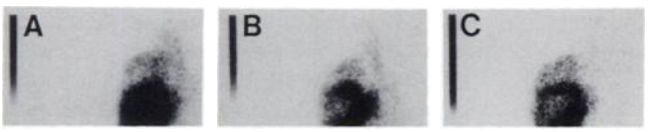

FIGURE 6. Serial ^{99m}Tc-teboroxime myocardial images following high-dose adenosine stress without occlusion (A), and after high-dose adenosine stress with severe partial LAD stenosis 1 min postinjection (B) and at 5 min postinjection (C). The latter two images demonstrate clear evidence of relative defect "redistribution" phenomenon in the anteroseptal perfusion defect. Data from the same animal are quantitatively displayed in Figure 2. This "redistribution" phenomenon was present in 60% of high-dose adenosine plus LAD stenosis studies.

Blood Clearance Kinetics. Previous animal studies (*5, 23*) have demonstrated rapid blood clearance of ^{99m}Tc-teboroxime after intravenous injection, with no difference in baseline and dipyridamole blood kinetics. In previous clinical studies, rest injection blood levels decrease from 39% of the injected dose at 90 sec to only 9.5% at 15 min (*1*). Residual blood ^{99m}Tc-teboroxime activity in dogs at rest and after dipyridamole stress averages 8% ± 3% of peak at 2 min and 4% ± 2% at 5 min (*5*). Blood-pool clearance data were acquired in the current study throughout imaging (30 min) to examine the input function at baseline and following adenosine and dipyridamole stress. These data indicated rapid biexponential blood-pool clearance of the agent under each experimental condition and confirmed that blood-pool background activity did not significantly affect myocardial imaging beyond 2 min postinjection (Fig. 3). Early blood ^{99m}Tc-teboroxime clearance kinetics were comparable and significantly different from control following dipyridamole and adenosine stresses.

Experimental Limitations

Coronary Stenosis Model. The severe (>90%) partial coronary stenoses utilized in these studies (*19*) predictably reduced the coronary flow reserve to markedly abnormal levels, although a range of abnormality was possible (*14, 18*). In contrast to human angioplasty (*24*), in awake or anesthetized animals coronary flow increases in nonoccluded perfusion beds during contralateral coronary artery occlusion (*25*). No attempt was made in the current study to utilize pharmacologic neuronal blockade, thus the potential existed for reflex contralateral hyperemia with single coronary artery occlusion in these studies. Coronary flow in the contralateral unoccluded bed remains unchanged during pacing "demand" stress compared to control conditions (1.4–1.5 ml/min/g) in our model (*19*).

Pharmacologic Stress. Both pharmacologic agents utilized in the current study have profound, dose-dependent effects on coronary blood flow, which plateau at the highest doses administered (*15–18*) and preferentially alter subendocardial perfusion (*15,16*). Despite reflex changes in systemic blood pressure (*27*) and cardiac index (*29*), intravenous vasodilator administration does not alter intrinsic left ventricular function in normal individuals (*28*) or dogs (*13*).

In the current study, near-maximal vasodilatation was achieved by both high-dose adenosine and dipyridamole at similar doses to those in previous studies (*13,27–29*) without associated significant global or regional LV functional effects in the absence of coronary occlusion. Poststenotic reactive hyperemia may have accelerated clearance in these beds (*30*), potentially reducing the differences

observed between normal and post-stenotic clearance kinetics. Significant differences in teboroxime clearance were noted, despite this potential but transient confounding effect.

Qualitative-Quantitative "Redistribution" Concordance. The 60% concordance between qualitative and quantitative relative "redistribution" for the different stresses studied represents the relationship between images that showed unequivocal evidence of "redistribution" by both analytic methods. The rapid clearance of the ^{99m}Tc-teboroxime from the canine myocardium made qualitative evaluation of perfusion defects beyond 5 min difficult in 20% of studies due to low count rates. This resulted in lower rates of qualitative "redistribution" (54%) as compared to the more rigorous quantitative curve analysis (71%). The approach of ^{99m}Tc-teboroxime counts to within 40% of their original difference in the unoccluded and post-stenotic zones might not have been visually appreciated, even by experienced observers (corresponding to a normal versus defect zone counts ratio of 1.67).

Background Subtraction. Different background activity contributions from the splanchnic and pulmonary regions may confound the evaluation of static planar images of tracers with significant hepatic uptake such as ^{99m}Tc-sestamibi (*22,26*), ^{201}Tl (*12*), ^{123}I-phenyl pentadecanoic acid (*10*) and meta-iodobenzyl guanidine (*9*). Planar ^{99m}Tc-sestamibi images differ from ^{201}Tl images due to their marked subdiaphragmatic uptake (in liver, gallbladder, intestinal tract) and decreased low-photon energy scatter (*22*). These features are also noted in ^{99m}Tc-teboroxime images (*4,5,30*), which are characterized by spatially and temporally inhomogeneous background activity. Blood-pool predominates early following injection (0–1 min), with a gradual increase in lung activity (low level) and splanchnic activity (high level) by 5–10 min postinjection. To address this difficult problem in the current dynamic imaging study of ^{99m}Tc-teboroxime kinetics, two background ROIs were placed at the level of the heart well above the diaphragm and secondary hepatic counts. Averaged activity in one blood pool and one lung ROI were used to correct for spatially and temporally variable background effects in each image frame. Based on examination of our raw time-activity data and previously reported experimental (*31*) and clinical data (*4,5,23*), an early (1–11 min) myocardial washout rate was calculated.

The use of two blood-pool regions (aorta and LV cavity) caused oversubtraction of counts from early images, and inadequate background subtraction in later images. The use of lung only ROIs was insufficient for background subtraction of early images. A narrow range of early (5 min) lung-to-heart ^{99m}Tc-teboroxime ratios followed disparate hemodynamic stresses. Correction for temporally variable background activity was prospectively performed prior to analysis of myocardial clearance kinetics following coronary hyperemic and ischemic stresses, revealing a perfusion defect in 85% of studies.

Interpolative background subtraction methods have been used to correct for high secondary lung and splanchnic counts in static planar ^{99m}Tc-Sestamibi studies (*22*), but would be difficult to apply to the 40 frame dynamic planar imaging protocol utilized here. There are no data to confirm whether splanchnic uptake of ^{99m}Tc-teboroxime, a potential confounding effect in inferoapical perfusion beds (*2,4*), varies at different workloads or under the effect of coronary hyperemia. A modified interpolative background subtraction technique will be required to optimize ischemia detection in standard static planar ^{99m}Tc-teboroxime images.

Standard rotational tomographic imaging reduces the problem of overlying background activity, but depends on a relatively stable tracer concentration in the myocardium over the acquisition time. The rapidly cleared ^{99m}Tc-teboroxime agent may be tomographically studied with multiple head camera systems that reduce imaging time.

Clinical Implications

These data provide important insights into the clinical potential for combining nonexercise cardiac stresses with myocardial ^{99m}Tc-imaging. In a previous clinical study (*15*), 80% of ^{99m}Tc-teboroxime perfusion defects were found to be distal to high grade (>90%) stenoses similar to those in this experimental protocol. Our studies, performed under a variety of nonexercise maximal stress conditions, demonstrated comparable sensitivity (62%), high specificity (100%) and overall diagnostic accuracy of 81% for detecting regional ischemia based on myocardial tracer clearance rates. By extrapolating these data to a clinical setting, optimum pharmacologic stress (dipyridamole 0.56 mg/kg or adenosine 160 μg/kg/min) or transesophageal pacing would have correctly identified 60% of post-stenotic zones, with no false-positive studies. Inclusion of additional studies with qualitatively graded visual "redistribution" increased sensitivity to 80%.

The potential clinical applicability of this analysis of dynamic teboroxime clearance (disappearance) for evaluation of functional perfusion abnormalities in patients with defined coronary anatomy is implied. Studies of ^{99m}Tc-teboroxime in coronary artery disease patients using an exercise-rest imaging protocol have also demonstrated that dynamic early (5–10 min) postexercise imaging detects "redistribution" in 82% of initial perfusion defects (*2*). Our description of early postinjection relative ^{99m}Tc-teboroxime "redistribution" by qualitative and quantitative analysis in this study confirms these clinical observations and extends previous studies by demonstrating this phenomenon during reperfusion after transient total occlusion and following nonexercise (pharmacologic and pacing) stresses. Further studies of maximal exercise and nonexercise stress will be required to determine whether less severe stenoses produce comparable post-stress defect visualization and relative "redistribution" to that observed in the current experimental study of severe coronary stenosis and occlusion-reperfusion.

ACKNOWLEDGMENTS

The authors thank Dr. Adrian Nunn (Bristol-Meyers-Squibb Institute) for his support, Mr. Daniel Escobedo for his expert technical assistance, Ms. Debbie Helterbridle for secretarial assistance and Dr. Tuhin K. Chaudhuri and Mr. John Straw, Division of Nuclear Medicine, Audie L. Murphy Veterans Administration Hospital, for expert radiopharmacy support. Supported in part by the American Heart Association (Texas affiliate) grant-in-aid (88G-355) and by the Bristol-Meyers-Squibb Institute, Princeton, NJ. Presented in part at the American Heart Association 63rd Annual Scientific Sessions, Dallas, TX, November 1990.

REFERENCES

1. Coleman RE, Maturi M, Nunn AD, Eckelman WC, Juri PN, Cobb FR. Imaging of myocardial perfusion with Tc-99m SQ30217: dog and human studies [Abstract]. *J Nucl Med* 1986;27:893–894.
2. Hendel RC, McSherry B, Karimeddini M, Leppo JA. Diagnostic value of a new myocardial perfusion agent, teboroxime (SQ30,217), utilizing a rapid planar imaging protocol: preliminary results. *J Am Coll Cardiol* 1990;16:855–861.
3. Herzog WR, Nys A, Cianci ML, Katz RJ, Keba RC, Wasserman AG. Planar and tomographic myocardial imaging with SQ30217, a new technetium-labeled agent [Abstract]. *J Am Coll Cardiol* 1989;13:98A.
4. Seldin DW, Johnson LL, Blood DK, et al. Myocardial perfusion imaging with technetium-99m-SQ30217: comparison with thallium-201 and coronary anatomy. *J Nucl Med* 1989;30:312–319.
5. Stewart RE, Schwaiger M, Hutchins GQ, et al. Myocardial clearance kinetics of technetium-99m-SQ30217: a marker of regional myocardial blood flow. *J Nucl Med* 1990;31:1183–1190.
6. Li QS, Solot G, Frank T, Wagner HN, Becker L. Serial tomographic myocardial perfusion studies with Tc-99m-SQ30217 at rest and during dipyridamole [Abstract]. *Circulation* 1988;78(suppl II):II–126.
7. Sodums MT, Badke FR, Starling MR, Little WC, O'Rourke RA. Evaluation of left ventricular contractile performance utilizing end-systolic pressure-volume relationships in conscious dogs. *Circ Res* 1984;54:731–739.
8. Badke FR, Boinay P, Covell JW. Effects of ventricular pacing on regional left ventricular performance in the dog. *Am J Physiol* 1980;238:H858–H867.
9. Glowniak JV, Turner FE, Gray LL, Polac RT, Lagunas-Solar MC, Woodward WB. Iodine-123-metaiodobenzylguanidine imaging of the heart in idiopathic congestive cardiomyopathy and cardiac transplants. *J Nucl Med* 1989;30:1182–1191.
10. Kennedy PL, Corbett JR, Kulkarni PV, et al. Iodine-123-phenylpentadecanoic acid myocardial scintigraphy: usefulness in the identification of myocardial ischemia. *Circulation* 1986;74:1007–1015.
11. Okada RD, Boucher CA, Kirshenbaum HK, et al. Improved diagnostic accuracy of thallium-201 stress test using multiple observers and criteria derived from interobserver analysis of variance. *Am J Cardiol* 1980;46:619–624.
12. Okada RD, Leppo JA, Boucher CA, Pohost GM. Myocardial kinetics of thallium-201 after dipyridamole infusion in normal myocardium and in myocardium distal to stenosis. *J Clin Invest* 1982;69:199–209.
13. Freeman GL, Colston JT, Hultman J. Influence of adenosine on left ventricular performance in conscious dogs. *Am J Physiol* 1990;258(part 2):H424–430.
14. Kirkeeide RL, Gould KL, Parsel L. Assessment of coronary stenoses by myocardial perfusion imaging during pharmacologic coronary vasodilatation. VII. Validation of coronary flow reserve a single integrated functional measure of stenosis severity reflecting all its geometric dimensions. *J Am Coll Cardiol* 1986;7:103–113.
15. Gerwitz H, Gross SL, Williams DO, Most AS. Contracting effects of nifedipine and adenosine on regional myocardial blood flow distribution and metabolism distal to severe coronary arterial stenosis: observations in sedated, close-chest domestic swine. *Circulation* 1984;69:1048–1057.
16. Rembert JC, Boyd LM, Watkinson WP, Greenfield JC. Effect of adenosine on transmural myocardial blood flow distribution in the awake dog. *Am J Physiol* 1980;239:H7–H13.
17. Wilson RF, Christensen B, Zimmer S, Laxson D, White CW. Effects of adenosine on the coronary circulation in humans. *J Am Coll Cardiol* 1989;13:132A.
18. Wilson RF, White CF. Intracoronary papaverine: an ideal coronary vasodilator for studies of the coronary circulation in conscious humans. *Circulation* 1986;73:444–457.
19. Applegate RJ, Walsh RA, O'Rourke. Comparative effects of pacing-induced and flow-limited ischemia: the effect of severity versus type of myocardial ischemia on diagnostic function. *Circulation* 1990;81:1380–1392.
20. Leppo JA, Meerdink DJ. Comparative myocardial extraction of two technetium-labeled BATO derivatives (SQ30217, SQ32014) and thallium. *J Nucl Med* 1990;31:67–74.
21. Grunwald AM, Watson DD, Holzgrefe HH, Irving JF, Beller GA. Myocardial thallium kinetics in normal and ischemic myocardium. *Circulation* 1989;64:610–618.
22. Koster K, Wackers FJT, Mattera JA, Fetterman RC. Quantitative analysis of planar technetium-99m-sestamibi myocardial perfusion images using modified background subtraction. *J Nucl Med* 1990;31:1400–1408.
23. Narra RK, Nunn AD, Kuczynski BL, Feld T, Wedeking P, Eckelman WC. A neutral technetium-99m complex for myocardial imaging. *J Nucl Med* 1989;30:1830–1837.
24. Feldman RL, Conti CR, Pepine CJ. Regional coronary versus flow responses to transient coronary artery occlusion in human beings. *J Am Coll Cardiol* 1983;2:1–10.
25. Joyce EE, Gregg DE. Coronary artery occlusion in the intact unanesthetized dog: intercoronary reflexes. *Am J Physiol* 1967;213:64–70.
26. Kiat H, Maddahi J, Roy L, Friedman J, Berman DS. Comparison of Tc-99m-methoxy-isobutyl with Tl-201 imaging by planar and SPECT techniques for assessment of coronary diseases. *Am Heart J* 1989;117:1–11.
27. Marchant E, Pichard A, Rodriguez JA, Casanegra P. Acute effect of systemic versus intracoronary dipyridamole on coronary circulation. *Am J Cardiol* 1986;57:1401–140.
28. Watt AH, Penny WJ, Singh H, Routledge PA, Henderson AH. Adenosine carries transient dilatation of coronary arteries in man. *Br J Clin Pharmacol* 1987;24:665–668.
29. Biaggioni I, Olafsson B, Robertson RM, Hollister AS, Robertson D. Cardiovascular and respiratory effects of adenosine in conscious man. *Circulation Res* 1987;61:779–786.
30. Leppo JA, Okada RD, Strauss HW, Pohost GM. Effect of hyperaemia on thallium-201 redistribution in normal canine myocardium. *Cardiovasc Res* 1985;19:679–685
31. Glover DK, Okada RD, Hebert CB. Tc-99m-teoboroxime (SQ30,217, Cardiotec) kinetics in normal and ischemic canine myocardium. *Circulation* 1990;82(suppl III):III–486.